PEM Electrolysis in a Stirred-Tank Bioreactor Enables Autotrophic Growth of *Clostridium ragsdalei* with CO_2 and Electrons

Irina Schwarz[+],[a] Arielle Rieck[+],[b] Asad Mehmood,[b] Raphaela Bublitz,[a, b] Lukas Bongers,[a] Dirk Weuster-Botz,*[a] and Tim-Patrick Fellinger*[b]

Acetogenic bacteria produce CO_2-based chemicals in aqueous media by hydrogenotrophic conversion of CO_2, but CO is the preferred carbon and electron source. Consequently, coupling CO_2 electrolysis with bacterial fermentation within an integrated bio-electrocatalytical system (BES) is promising, if CO_2 reduction catalysts are available for the generation of CO in the complex biotic electrolyte. A standard stirred-tank bioreactor was coupled to a zero-gap PEM electrolysis cell for CO_2 conversion, allowing voltage control and separation of the anode in one single cell. The cathodic CO_2 reduction and the competing hydrogen evolution enabled *in-situ* feeding of *C. ragsdalei* with CO and H_2. Proof-of-concept was demonstrated in first batch processes with continuous CO_2 gassing, as autotrophic growth and acetate formation was observed in the stirred BES in a voltage range of −2.4 to −3.0 V. The setup is suitable also for other bioelectrocatalytic reactions. Increased currents and lower overvoltages are however required. Atomically-dispersed M–N–C catalysts show promise, if degradation throughout autoclaving can be omitted. The development of selective and autoclavable catalysts resistant to contamination and electrode design for the complex electrolyte will enable efficient bioelectrocatalytic power-to-X systems based on the introduced BES.

1. Introduction

Reducing emissions of greenhouse gases like CO_2 is a major demand for mankind to reduce the effect of climate change. In this context great interest has emerged in biological CO_2-fixing processes which are able to effectively convert CO_2 emissions into multi-carbon organic chemicals and may therefore open the door for the establishment of a circular carbon economy.[2] Acetogenic bacteria are able to produce CO_2-based chemicals in aqueous media by autotrophic conversion of CO_2 with high energetic efficiency of up to 70–90%.[3] The reductive acetyl-CoA pathway of acetogens can be supplied with both, electron carriers such as H_2 and CO[4] or directly with electrons from a cathode.[5] The direct electrochemical CO_2 reduction via electrolysis is another promising approach and different companies have already established demonstration reactors or pilot plants.[6] Generally, CO_2 electrolysis has two main commercially desirable scenarios. First, the production of syngas (CO/H_2O) for subsequent methanol production and second, direct electrosynthesis of value-added organic chemicals such as acetate or alcohols.[7] Those scenarios require a narrow stoichiometry window of the syngas components and value-added products would be desirable in high purity. So far, those requirements are only obtained using elaborate separation technology, which is not conformed with a decentralized industrial conversion of CO_2 scrubbed from the atmosphere.[7b] Alternatively, catalysts with high selectivity at operating conditions would be required. However, the electrochemical CO_2 reduction in aqueous electrolytes has low selectivity between the generation of formate, CO and hydrocarbons if long-time operation or flexibility in the electrolyzer performance are considered.[8] Due to the competition with the water splitting reaction occurring in the same potential range, furthermore H_2 is produced.

Consequently, an artificial photosynthesis approach of coupling CO_2 electrolysis with bacterial fermentation, in which bacteria are tolerant to different reduction equivalents (stoichiometry insensitive) is promising. Traditionally 'H-cell' reactors are used in the lab for studying bioelectrochemical CO_2 reduction with acetogens.[9] The anode and cathode chambers are separated with a selective polymer electrolyte membrane (PEM), while limiting oxygen diffusion from the anode chamber to avoid both abiotic consumption of electrons at the cathode and poisoning of the strictly anaerobic acetogens in the cathode chamber.[10] The microbial electrosynthesis reactor design can be simplified if the anode is installed at the top of an upstanding tubular reactor and the cathode with biofilm at

[a] *I. Schwarz,[+] R. Bublitz, L. Bongers, Prof. Dr. D. Weuster-Botz*
Chair of Biochemical Engineering, TUM School of Engineering and Design, Technical University of Munich (TUM)
Boltzmannstraße 15, 85748 Garching bei München, Germany
E-mail: dirk.weuster-botz@tum.de
Homepage: https://www.epe.ed.tum.de/biovt/

[b] *A. Rieck,[+] Dr. A. Mehmood, R. Bublitz, Dr. T.-P. Fellinger*
Division 3.6, Electrochemical Energy Materials, Bundesanstalt für Materialprüfung und -forschung (BAM), Unter-den-Eichen 44–46, 12203 Berlin, Germany
E-mail: tim-patrick.fellinger@bam.de
Homepage: https://www.bam.de/

[+] *Irina Schwarz and Arielle Rieck share the first authorship.*

Supporting information for this article is available on the WWW under https://doi.org/10.1002/celc.202300344

the bottom. This configuration avoids oxygen exposure to the cathode allowing to remove the membrane separating anode and cathode.[10] Recent considerations suggest that gas-diffusion electrodes for the anode reaction, directly coupled to the bioreactor, separated by the PEM may be the most promising cell configuration, as the cathode would allow high current densities, hence not be limiting.[11]

Stirred-tank electrobioreactors were recently introduced because the standard bioreactor in bioprocess development is an ideally mixed stirred-tank reactor which enables full control of the reaction conditions (e.g. pH, T, power input, gas-liquid mass transfer) with batch, fed-batch or continuous operation.[12] Standard lab-scale stirred-tank bioreactors made of glass were previously modified by electrical insulation of the electrodes and all parts meeting the liquid phase (stirrer, baffles), by adding cathode, anode and reference electrodes via standard ports at the lid and by insertion of an installation to generate two separate chambers.[1]

In this work we present an integrated bio-electrocatalytical system (BES) consisting of a 2 L stirred-tank bioreactor coupled to a zero-gap PEM electrolysis cell for the electrolytic CO_2 conversion utilizing the cathodic CO_2 reduction reaction (CO_2RR). Within this system the reaction products of both CO_2RR as well as the competing hydrogen evolution reaction (HER) at the cathode (CO and H_2) are directly fed to acetogenic bacteria within the ideally mixed bioreactor which can convert them as carbon and electron source via the reductive acetyl-CoA pathway to carbon compounds (e.g., alcohols and acids). The anode reaction is equivalent to PEM water electrolysis cell, allowing high current densities. Due to the direct contact of cathode catalyst and bacterial medium, the catalysts must not be bactericidal and for the reasons of cost-effectiveness, precious metal-based catalysts should be avoided.

Dirk Weuster-Botz studied Chemical Engineering in Karlsruhe followed by his doctorate at the Institute of Biotechnology (IBT) of the Research Center Jülich. As Postdoc at the IBT he established a junior research group on fermentation science. After an industrial research stay at DSM, Netherlands, he earned his postdoctoral lecture qualification at RWTH Aachen followed by his appointment as full professor of Biochemical Engineering at the Technical University of Munich. With a team of ~30 scientists he works on better understanding and scale-up of microbial bioprocesses. 2012 he was appointed as member of the National Academy of Science and Engineering (acatech).

Tim Fellinger studied Nanostructure and Molecular Science in Kassel followed by a PhD in Colloid Chemistry at the University of Potsdam. With postdoctoral stints at Tokyo Institute of Technology (TiTech) and Chalmers Institute of Technology in Gothenburg he was a research group leader with Prof. M. Antonietti at the Max-Planck Institute for Colloids and Interfaces (MPIKG) and at the Chair for Technical Electrochemistry (Prof. H. Gasteiger) at TUM. At BAM he is Head of Division 3.6 Electrochemical Energy Materials with a research focus on chemistry and application of carbon-related active materials for energy storage and conversion.

Arielle Rieck studied Chemistry at the Freie Universität Berlin, majoring in organic chemistry. During her master's thesis she investigated the NHC-catalysed Norrish Type-II reactions. Afterwards, she started as doctoral candidate at the Bundesanstalt für Materialforschung und -prüfung (BAM). Here, her research focuses on developing biocompatible catalysts for electrochemical reactions such as the CO_2RR.

Irina Schwarz studied Industrial Biotechnology at the Technical University of Munich (TUM), where she investigated first metabolic burden through heterologous protein production in yeast during her master's thesis at the professorship Systems Biotechnology. Afterwards, she started her research on bioelectrocatalysis with acetogenic bacteria at the Chair of Biochemical Engineering (TUM) to work as a doctoral candidate.

Asad Mehmood received his bachelor's degree in Physical Chemistry from Quaid-i-Azam University, Pakistan, and PhD in Energy and Environmental Engineering from Korea Institute of Science and Technology (KIST), South Korea. During his PhD, he worked with electrocatalysts and membrane electrode assemblies for low temperature fuel cells. His current research is mainly focused on the development of carbon-based materials for electrochemical energy conversion and storage systems. At BAM, he is involved in the development of precious metal-free catalysts for electrochemical conversion reactions such as oxygen reduction and CO_2 reduction.

2. Results and Discussion

2.1. Reactor design

The novel BES consists of a 2 L cylindrical reaction vessel with heat exchanger combined with a stainless-steel lid normally used for standard stirred-tank bioreactors, and at the bottom connected to a custom-made PEM electrolysis single cell. The cathode faces the bioreactor, while the PEM separates cathode and bioreactor from the anode. For electrical insulation, the agitator shaft of the reaction vessel is made of polyetheretherketon (PEEK) and equipped with two Rushton turbines. Insulated baffles are applied in the reaction vessel. The insulated sparger for dispersion of the gas phase (CO_2) in the fermentation medium was mounted above the cathode surface (Figure 1a). Temperature, pH, stirrer speed and CO_2 volume flow were fully controlled, and redox potential was monitored by a probe in addition. Through an Ag/AgCl reference electrode immersed in a salt bridge (electrolyte: 3 M KCl, frit distance from cathode ≈ 10 cm), cathode and anode potential were measured. The PEEK bottom end-plate is mounted by a flange and integrated with an electrolysis single cell (Figure 1b). Directly in contact to the end-plate is a titanium current collector (Figure 1b (C)) providing electrical contact to the cathode catalyst layer. To ensure tightness between the end-plate and the current collector, a round O-ring sealing is used (Figure 1b (B)). Similarly, a second O-ring sealing is used between the end-plate and the reactor to ensure tightness (not shown). The end-plate has a 5 cm^2 round opening which is connected to the catalysts layer through a perforated cathode current collector (geometrical pore surface area of A_{geo} = 1.2 cm^2). The catalyst layer is connected to the bioreactor volume via a conical opening in the end plate ending in round 5 cm^2 interface with the cathode electrode. The membrane-electrode-assembly (MEA) consists of a 4.5 cm×4.5 cm carbon paper cathode (SGL22B©) with 5 cm^2 active area coated with a homemade precious metal-free Zn/Co–N–C catalyst (Figure 1b-(D)), a Nafion© PEM membrane (Figure 1b(E)€) and a commercial Ir/IrO_x anode catalyst coated onto a titanium mesh (Figure 1b(F)). The anode catalyst layer is connected to a Ti serpentine flow field (Figure 1b(G)) and a Ti current collector (Figure 1b(H)) as in H_2-O_2 electrolysis cells, compressed via the final PEEK end-plate (Figure 1b(I)) with stainless steel threaded rods (Figure 1b(J)).

2.2. Cathode catalyst and electrodes

The technological viability of the bacteria-assisted electrolysis depends on the usage of efficient, earth abundant, biocompatible, and selective electrocatalysts. Currently, scarce catalysts such as Ag and Au are used for the CO_2RR, although copper-based catalysts also show promising activity.[13] However, these precious metal catalysts may hamper the use of decentral CO_2 conversion technology for cost reasons, because of their bactericidal properties. As an alternative, specific single-atom catalysts, so-called atomically dispersed M–N–C catalysts are of great interest. Those catalysts are originally enzyme-inspired and comprise nitrogen-coordinated metal ions as active catalytic sites. In contrast to enzymes, the active sites are not embedded into a protein scaffold, but into an electrically conductive and chemically resistant carbon matrix.[14] Hierarchically porous carbon backbones are preferred since they combine high surface area, hence good catalyst dispersion, and a mass-transport enabling pore system. As a cathode catalyst for the BES a zinc and cobalt containing catalyst (Zn/Co–N–C) is prepared with a method developed in our group.[15] Through carbonization of a zinc-containing metal-organic framework precursor (ZIF-8) first an Zn–N–C single-atom material is obtained. Partial exchange of zinc with cobalt via transmetallation produced a Zn/Co–N–C catalyst (for the detailed preparation see methods). Nitrogen sorption porosimetry of Zn/Co–N–C catalyst revealed a micro-meso-macroporous material which is advantageous for mass-transport through the catalysts

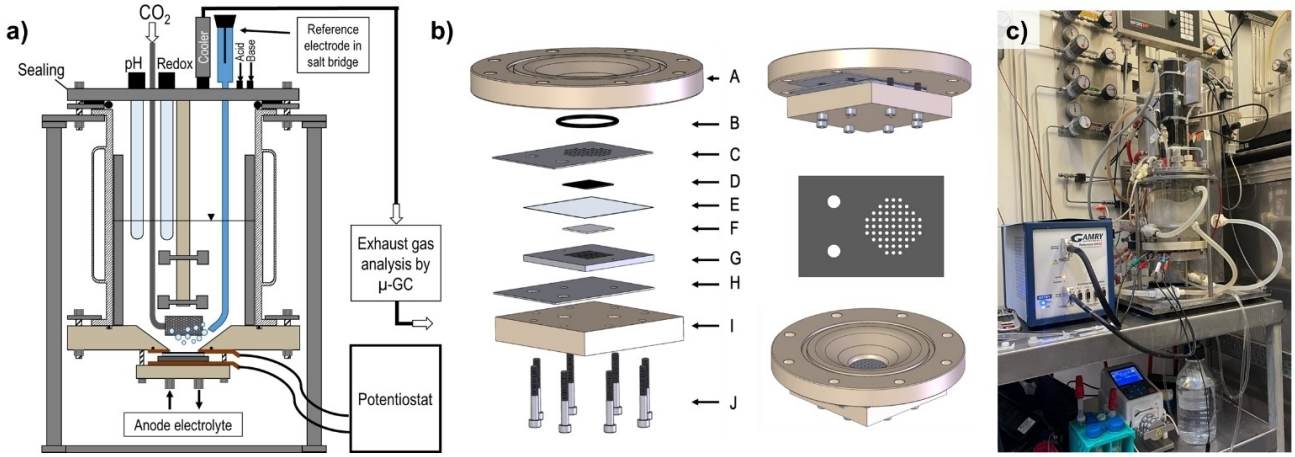

Figure 1. (a) Design of a bio-electrocatalytical system (BES) comprising directly coupled stirred-tank bioreactor and PEM electrolysis cell at the bottom plate. (b) explosion sketch of disassembled electrochemical system connected to the bioreactor bottom plate (A: PEEK bottom plate, B: O-ring, C: Ti current collector, D: cathode catalyst layer, E: Nafion© membrane, F: anode catalyst layer, G: Ti flow field, H: Ti current collector, I: PEEK end-plate, J: screws), sketches of assembled cell and top-view of cathode current collector, (c) photograph of running stirred BES in the lab.

layer and to the active sites within the layer (Figure S1). The high specific surface area (SSA) of 1040 $m^2 g^{-1}$ and porosity of 55% is beneficial for an efficient accessibility to active sites. Scanning electron microscopy (SEM) imaging shows the pseudo-crystalline morphology of the Zn/Co–N–C catalyst particles (Figure 2a), which retain the precursor geometry throughout carbonization and ion-exchange. Particle sizes are between 50–200 nm resulting in a disordered packing and the resulting interstitial mass-transport porosity. X-ray photoelectron spectroscopy (XPS) analysis was used to investigate the catalyst composition. The survey spectrum reveals a nitrogen content of ≈14.65 at.%N and a metal content of 2.97 at.% (0.54 at.%Co and 2.43 at.%Zn) (Figure S2). High resolution N1s spectra show five different types of nitrogen species (Figure 2b) and their relative abundance. The nitrogen-doping within the carbon backbone is predominantly functionalized with terminal pyridinic groups (398.2–398.8 eV, 56%), which can be related to the high surface area. The second highest fraction is metal-bound (399.4–400 eV, 21%) suggesting a good dispersion of the metal, largely in the form of single atom sites (for more details, see SI). The catalyst was first tested for CO_2R activity by means of rotating disc electrode (RDE) tests, showing high activity and selectivity towards CO_2R versus the competing HER (Figure S3).

Cathode catalyst coating on SGL22B© carbon, and anode catalyst coating using commercial Ir/IrOx powder on a commercial titanium fiber support were targeting respective catalyst loadings of 2 mg cm^{-2}. Successful cathode coating is evident from homogeneous surface structure observed by SEM (Figure 2c) and the Co and Zn signals measured on the coated support materials (white box in Figure 2c) using energy dispersive X-ray spectroscopy (EDX) measurements (Figure S4). A uniform dispersion of the anode catalyst is observed on the titanium fiber support, with an expected local concentration at the contact areas of different fibers (Figure 2d). EDX measurement performed on the anode (white box in Figure 2d) confirmed the presence of Ir catalyst (Figure S5).

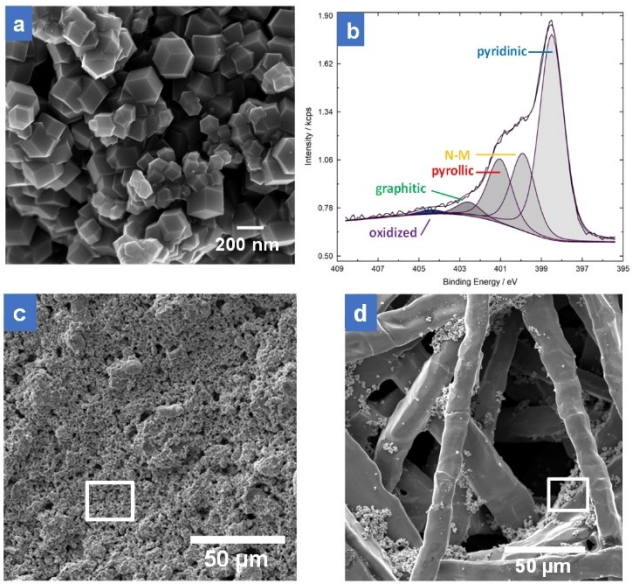

Figure 2. (a) SEM images of Zn/Co–N–C cathode catalyst, (b) high resolution N1s XPS spectrum of Zn/Co–N–C catalyst, and SEM images of coated (c) cathode and (d) anode with marked location of EDX measurements shown in Figure S4 and S5.

2.3. Single cell tests

In preparation of the proof-of-concept tests of the BES, we first tested the catalyst performance recording polarization curves from potentiostatically measured single points between −1.4 and −2.6 V in a homemade 5 cm^2 electrolysis single cell (see methods) using 0.5 M $KHCO_3$ electrolyte at RT (Figure S6). HER activity was investigated in N_2-saturated electrolyte, which can be considered as background for the CO_2R activity test in CO_2-saturated electrolyte. The expected exponential current-voltage relations are indicative of electrocatalytic processes. Significantly increased current was observed in the CO_2R test, for instance −48 mA in CO_2-saturated electrolyte *vs* −33 mA in N_2-saturated electrolyte at −2.4 V. The comparative polarization curves are indirect proof of successful CO_2 conversion. Correction for resistive voltage loss (iR-correction) reveals insignificant changes reflecting a relatively small high-frequency resistance (HFR) of the cell (≈0.6 Ω) (comparison in Figure S7) compared to common bioelectrochemical cells. Compatibility of the catalysts with the fermentation medium (phosphate electrolyte containing yeast extract, chloride salts, vitamins, etc.) used in the BES to grow bacteria is critical for the successful integration of bioreactor and electrochemical cell. Single cell tests with the medium as electrolyte again show exponential current-voltage relation as well as significantly increased currents of up to 65% in CO_2-saturated electrolyte (e.g. −2.23 mA in CO_2-saturated electrolyte *vs* −0.77 mA in N_2-saturated electrolyte at −1.8 V) as an indirect proof of successful CO_2 reduction in this voltage range (Figure 3a). Interestingly, the CO_2 reduction onset is herein observed at 200 mV lower cell voltage (above ≈−1.8 V) as compared to the CO_2R onset in 0.5 M $KHCO_3$. Overall, reduced total currents of up to −45 mA were observed mainly contributed by lower HER, indicating undesirable interaction of the medium with electrode components. Overall, significant production of reduction equivalents with up to 65% selectivity towards CO_2 reduction can be expected from single cell tests. As previously observed by Haas et al. (2018), small voltages are optimal for CO_2 conversion while the ratio of CO_2R and HER currents (i_{CO}/i_{H2}) linearly drops with increasing voltage (Figure 3b).[7b] The current ratios i_{CO}/i_{H2} and i_{CO}/i_{total} in Figure 3b are herein derived from the deviating currents in N_2- vs. CO_2-saturation according to $i_{CO}/i_{H2} = (i_{CO2} - i_{N2})/i_{N2}$ and $i_{CO}/i_{total} = (i_{CO2} - i_{N2})/i_{CO2}$. The potentiostatic measurements of each point in the polarization curve can be found in the SI (Figure S8). Therein a continuously dropping current is apparent (points were recorded after t = 590 s). As commonly observed for CO_2 reduction, the initial current can be recovered by voltage pulses (herein not shown), to reduced polarization, which will be relevant later in the BES section.[16]

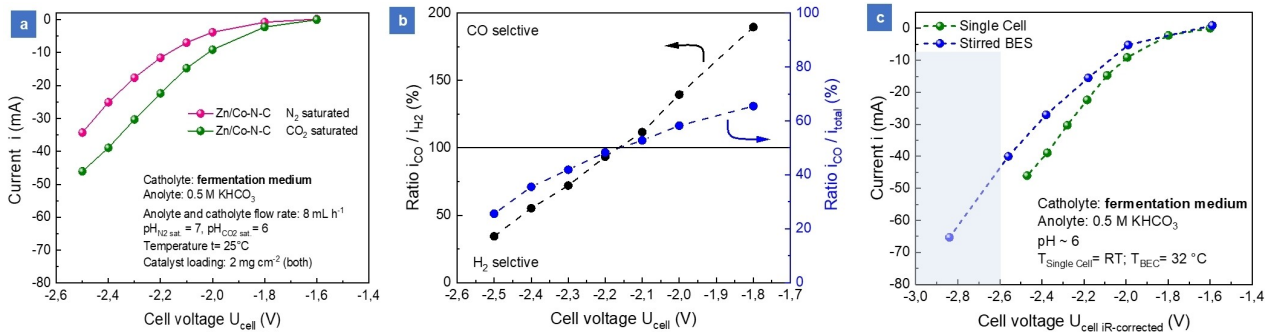

Figure 3. (a) Polarization curves in N_2 and CO_2-saturated fermentation medium as catholyte in 5 cm^2 single cells. (b) calculated current ratio and CO_2R selectivity of single cell tests, (c) comparison of single cell and stirred BES tests in abiotic fermentation medium electrolyte.

2.4. Bioelectrocatalytical system (BES) polarization

Transfer of the electrolysis cell operation in connection to the bioreactor in one BES may cause several challenges: The autoclaving of the BES, the turbulent medium and direct contact to bacteria may deteriorate the catalyst or catalyst support. The removal of the flow field on the cathode may lead to less homogenous/undefined mass transport and compression, and the contact to the current collector is required outside the active electrode area. Therefore, a first BES test was carried out with the abiotic fermentation medium as catholyte and at the cultivation temperature of $T_{BES} = 32\,^{\circ}C$ and pH 6.

To see if the performance in the PEM electrolysis single cell can be transferred into the BES, a comparison is done in Figure 3c. Achieving equivalent currents in the BES required applying significantly higher voltages. Considering the Ohmic cell resistance (iR-correction) does not significantly change the voltage difference required ($HFR_{BES} < 1\ \Omega$), so another resistance needs to cause the additional overvoltage (see Figure S8). Interestingly, even at high voltage, there is no indication of catalyst degradation in the BES. Although the BES was controlled via applied cell voltages between anode and cathode (2-electrode configuration to compare to single cell measurements), the electrode potentials were additionally determined in a secondary circuit with a Ag/AgCl reference electrode (see methods). The calculated anode and cathode potentials reveal larger polarization of the anode at constant current increase (Table S1).

An alternative anode reaction to the oxygen evolution reaction would therefore be one option to reduce the total cell voltage and hence increase energy efficiency. The additional overvoltage compared to single cell tests however indicates an additional resistance at the cathode side. The sheet resistance of the Toray paper on the cathode support is in the range of $R_{e,sheet} = 1–10\ \Omega$, which is too low to cause the observed overvoltage. From the slope of the deviating polarization curves of single cell and BES, it is apparent that the resistance ($R = \triangle U/\triangle I$) is not constant and therefore apparently not only Ohmic in nature.

Potentiostatic BES batch operation show higher CO-selectivity at smaller voltages, however, relatively high current densities are needed to measure partial pressures of evolving gases and to be able to allow significant bacterial growth for a 1 L batch cultivation of *C. ragsdalei*. Therefore, the voltages higher than −2.4 V were identified for operation (grey area in Figure 3c).

2.5. Potentiostatic stirred BES batch operation

Potentiostatic operation (chronoamperometry) of the BES was first investigated in abiotic conditions (without inoculation of *C. ragsdalei*) at three different constant voltages of −2.4, −2.8 and −3.2 V (Figure 4). At the same time, partial pressures of H_2 and CO in the exhaust gas were measured on-line by a micro gas chromatograph (μ-GC). The high total CO_2 concentration does not allow quantification of the relatively low CO_2 consumption.

Due to a delay period at the CO_2 gas flow rate chosen and the high gas volume of the BES including tubing, hydrogen gas and CO reached partial pressures of around 1 mbar after a process time of 1 h at a constant potential of −2.4 V (Figure 4a), but started to decrease correlating with a current flow reduction from −30 mA to −12 mA. Applying higher voltages of −2.8 V and −3.2 V increased current flows and, therefore, the p_{H2} and p_{CO}. After 8 h, the p_{CO} reached a maximum of 3.7 mbar, and the p_{H2} was 2.5 mbar at the maximum. Hydrogen gas production was preferred at higher potentials since p_{H2} achieved a higher maximal value of 5.3 mbar H_2 compared to 5.1 mbar CO.

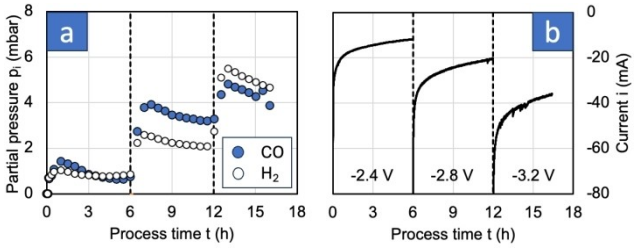

Figure 4. Electrocatalytical H_2 and CO production with a Zn/Co–N–C catalyst in the stirred BES without inoculation with *C. ragsdalei* is shown. The detected H_2 and CO gas is shown, illustrating relatively high CO selectivity between 6 and 12 h process time (a). A constant voltage of −2.4 V was applied between anode and cathode in the beginning and then elevated in two steps up to −2.8 V and −3.2 V (anaerobic fermentation medium, $T = 32\,^{\circ}C$, pH 6, $V = 1$ L, $n = 1200\ min^{-1}$, $F_{in,CO2} = 1.5\ L\,h^{-1}$). The corresponding polarization curves (b) show characteristic current decay with time.

It is worth noting, that the geometric electrode areas for HER ($A_{geo,\ HER} \approx 5\ cm^2$) and CO2R ($A_{geo,CO2} \approx 1.16\ cm^2$) are deviating and still a relative selectivity for CO2R is reached at −2.8 V cell voltage.

For biotic operation, the BES was assembled a second time and first operated in abiotic conditions (without inoculation of *C. ragsdalei*) at a constant voltage of −2.4 V for 2 h, then the potential was increased to −2.5 V (Figure 5). After 2.4 h, the BES was inoculated with *C. ragsdalei*. Regarding the process time from 2–8 h (Figure 5a), total current flows were similar compared to the abiotic test described before (Figure 4b, 0–6 h). A hydrogen gas partial pressure of 1.7 mbar was established after 4 h and stayed almost constant for further 7 h (Figure 5b). The partial pressure of CO reached 3 mbar after 5 h and decreased with decreasing current flow.

The initial redox potential in the bioreactor, which was tracked within the stirred BES using a redox-probe (Figure 5c), started with a value of +50 mV and decreased due to CO and hydrogen gas production to −25 mV before inoculation. Directly after inoculation the redox potential fell below −100 mV. But shortly afterwards, the increase of the redox potential to −25 mV and the decrease of the OD_{600} indicated dying of a part of the bacteria up to a process time of 19 h. Growth of the bacteria was observed and quantified by optical density (OD_{600}) measurements that can be referred to cell dry weight (CWD) concentrations (Figure 5d).

At a process time of 21 h, the potential was increased to −2.6 V and the repetitive regeneration of the cathode was started by applying +0.7 V every 3 h for 2 minutes to increase the current as observed in previous single cell tests (see above). The CDW concentration stayed constant until a process time of 42 h when the bacteria started to grow, reflected by a drop of the redox potential in correlation with biomass production. Applying the electrochemical regeneration method, maximal partial pressures of 5.7 mbar CO and 2.7 mbar H_2 were achieved after 30 h at a current flow higher than −15 mA, and stayed constant for 6 h. After 36 h, electrocatalytic activity diminished as current flows decreased to −8 mA resulting in a concomitant decrease of p_{CO} and p_{H2}. In addition, the continuous reduction of the partial pressures is caused by the consumption of the gases by *C. ragsdalei* when growth started at 42 h.

At a process time of 48 h, the potential was increased to −2.7 V to compensate for the ongoing current flow loss, but current flows were only slightly and temporarily restored (Figure 5a). Despite of low current flows, the in total produced CO and H_2 were sufficient for *C. ragsdalei* to grow with a specific exponential growth rate of 0.16 h^{-1} (exponential fit between 42–52 h, $R^2 = 0.99$). The acetate formation rate of 1.8 mg L^{-1} h^{-1} is low compared to biomass formation. This indicates preferred use of acetyl-CoA for the growth of *C. ragsdalei* due to CO consumption which results in increased ATP-formation compared to H_2/CO_2-consumption.[17] Eventually, an acetate concentration of 0.103 g L^{-1} is reached corresponding to an acetate

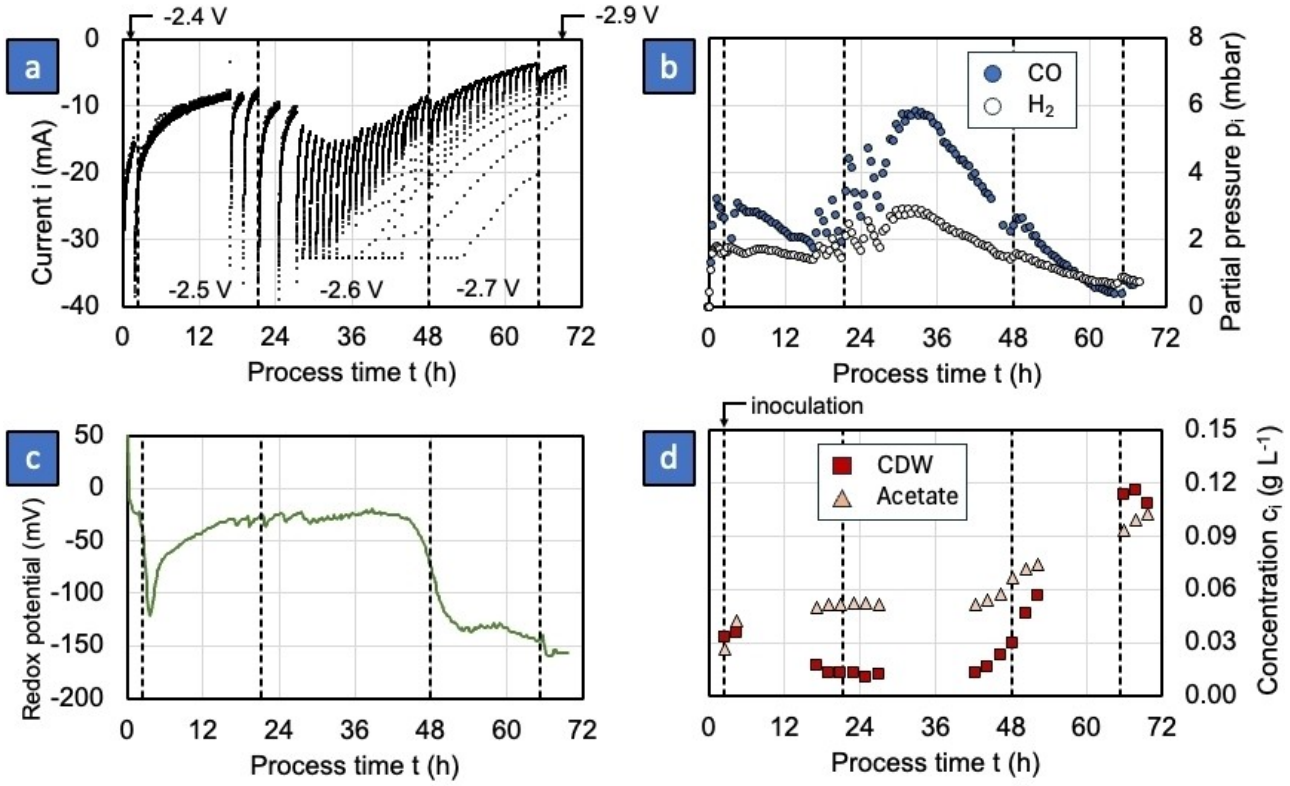

Figure 5. Bioelectrocatalytical batch conversion of CO_2 by *Clostridium ragsdalei* in the BES with CO and H_2 electrocatalytically produced at a Zn/Co–N–C catalyst (inoculation after 2.4 h). A potential of −2.4 V was applied between anode and cathode initially, afterwards the potential was increased to −2.5 V, −2.6 V, −2.7 V, and −2.9 V (a), and was controlled by the potentiostat. From 24 to 48 h, every 3 h a potential of +0.7 V were applied for 2 minutes to regerate the cathode. Process conditions: Anaerobic fermentation medium, T = 32 °C, pH 6, V = 1 L, n = 1200 min^{-1}, F_{in}, CO_2 = 1.5 L h^{-1}.

formation rate of 0.73 mmol d^{-1}. Note, that in the current research system no circular gas flow is realized, so the bacterial gas uptake is limited by the saturation kinetics.

3. Summary and Outlook

An integrated bio-electrocatalytical system (BES) for the bioelectrochemical conversion of electricity into chemicals has been developed. The BES consists of a stirred tank bioreactor with a connected zero-gap polymer-electrolyte-membrane (PEM) single electrolysis cell at the bottom plate. The setup allows separation of one electrochemical cell compartment from the cultivation medium, while the other electrode is directly operated within the bioreactor. A reference electrode allows potential control in a 3-electrode mode, while the proximity of the sparger to the cathode electrode allows advantageous mass-transport kinetics (gas diffusion electrode). A Zn/Co–N–C CO_2 reduction electrocatalyst with preference for CO_2R versus HER at lower operation voltages was developed and employed for proof-of-principle experiments of PEM CO_2 and water electrolysis-assisted growth of *Clostridium ragsdalei*. As compared to the other BES, a relatively low Ohmic cell resistance of $R_{cell} < 1\ \Omega$ proves the potential of the setup to reach high production rates. The BES setup allows production of CO and H_2 with relative selectivity for CO at lower operation voltages and its utilization to grow *Clostridium ragsdalei* and produce acetate. Besides the need for improved total currents or mass transport limitation in general, one challenge is to eliminate unassigned voltage losses compared to single cell tests. The impact of the bacterial medium on the cathode electrode requires further investigation. Herein pulsed voltage application was required to recover sufficient currents, however this is also common in abiotic CO_2 electrolysis.

Experimental

Synthesis of Zn/Co-N-C electrocatalyst: In order to obtain a nitrogen-doped carbon framework containing abundant Zn-N_x sites (Zn–N–C) pyrolysis of commercial ZIF-8 (Basolite Z1200, Sigma Aldrich) was done in a quartz tube furnace at 900 °C in N_2 atmosphere (5.0 from Linde) with a heating rate of 5 K min^{-1} and a dwelling time of 1 h. Next, the Zn–N–C was leached in a 2 M aqueous HCl solution (TH.Geyer) for partial removal of Zn. For partial transmetalation with cobalt, 100 mg of the washed Zn–N–C powder and 4.53 mg of anhydrous Co(II)Cl_2 (99.7 % anhydrous, Alfa Aesar) were dispersed in 150 mL methanol. The dispersion was refluxed for 15 h followed by thorough washing in de-ionized water and further leached overnight in 0.5 M aqueous HCl to ensure complete removal of the physisorbed and loosely bound Co ions. Afterwards, the zinc/cobalt-coordinated catalyst (Zn/Co–N–C) was thoroughly washed with de-ionized water and lastly dried in a glass vacuum oven (Büchi) over night at 150 °C.

Morphological and physicochemical characterization: N_2 gas sorption was measured with a Quantachrome Autosorb iQ–C–XR porosimeter and the sample was outgassed at least for 12 h at 150 °C. ASiQwin software was used to calculate BET surface area. XPS measurements were performed with an AXIS Ultra DLD photoelectron spectrometer manufactured by Kratos Analytical (Manchester, UK). XPS spectra were recorded using monochromatized aluminum K_α radiation for excitation, at a pressure of approximately $5 \cdot 10^{-9}$ mbar. The electron emission angle was 0° and the source-to-analyzer angle was 60°. The binding energy scale of the instrument was calibrated following a Kratos Analytical procedure which uses ISO 15472 binding energy data. For peak fitting a sum Gaussian-Lorentzian function was used. A modified Tougaard background was used for background correction. The Morphology of the material was examined by a FlexSEM with EDX spectrometer (Hitachi 1000 High Technology Europe GmbH, Krefeld).

Electrochemical analysis in half-cell and electrolysis single cell configurations: Initial activity screening of the Zn/Co–N–C catalyst was carried out in a half cell configuration using a rotating disc electrode (RDE) setup. The catalyst ink was made using the ink recipe reported for ZIF-8 derived M–N–Cs by Mehmood et al.[15] Catalyst powder (3 mg) was mixed with 623 μL de-ionized water/isopropanol 1 : 1 and 32.4 μL of 5 wt.% Nafion suspension (Sigma-Aldrich) and sonicated for 30 min. From the prepared ink 8.56 μL was dropped onto the glassy carbon surface to achieve a catalyst loading of 0.2 mg cm^{-2}. The RDE measurements were carried out in CO_2 and N_2 saturated 0.1 M $KHCO_3$ electrolyte, at RT at a scan rate of 5 mV s^{-1}. LSVs were recorded at a rotation speed of 1600 rpm. The electrochemical single cell tests were carried out using a homemade electrolysis cell (BAM) with a graphite serpentine flow field at the cathode and a Ti serpentine flow field at the anode with copper current collectors. The cathode catalyst ink was prepared by mixing 10 mg Zn/Co–N–C catalyst powder, 240 μL de-ionized water, 304 μL of analytical grade 2-propanol (99.8 %, TH.Geyer) and 217 μL of 5 wt.% Nafion suspension (Sigma-Aldrich). The ink was sonicated for 30 min and then coated onto the carbon support (SGL22B, Fuel Cell store) by brush painting. The anode catalyst ink was prepared by mixing 10 mg of a commercial Ir/IrO_x powder (Fuel Cell store), 240 μL de-ionized water, 304 μL of analytical grade 2-propanol (99.8 %, TH.Geyer) and 26 μL of 5 wt.% Nafion suspension (Sigma-Aldrich). The Ir/IrO_x catalyst ink was coated on a Ti fiber (Fuel Cell Store) support by brush painting. The catalyst loading was 2.0 mg cm^{-2} for both electrodes with a geometric area of 5 cm^2. The membrane-electrode-assembly (MEA) was fabricated by hot pressing the catalyst coated cathode onto a Nafion 117 membrane (Fuel Cell store) for 3 min at 130 °C under an applied pressure of 2 bar. Ir/IrO_x coated Ti fiber anode was assembled with the MEA in single cell without hot pressing. For sealing and compression, glass-reinforced PTFE gaskets were used. The gasket thickness at the cathode was 340 μm and 190 μm at the anode, aiming at 20 % compression. Single cell measurements were conducted at room temperature (25 °C) by supplying 0.5 M $KHCO_3$ aqueous solution at the anode and N_2- or CO_2-saturated 0.5 M aqueous $KHCO_3$ solution or mineral fermentation medium at the cathode. The mineral medium itself is a complex, with 1 g L^{-1} aqueous yeast extract, 2.4 g L^{-1} NaCl, 3 g L^{-1} NH_4Cl, 0.3 g L^{-1} KCl, 0.3 g L^{-1} KH_2PO_4, 20 mg L^{-1} nitrilotriacetic acid, 11.2 mg L^{-1} manganese(II) sulfate monohydrate, 11 mg L^{-1} ammonium iron(II) sulfate-hexahydrate, trace elements (in the range of 1–5 mg L^{-1} and vitamins (in the 020–150 μg L^{-1} range). All experiments were carried out using a potentiostat (Gamry, Interface 1010). Pure CO_2 and N_2 gases (Linde) were used to record the potentiostatic polarization curves. The potentiostatic curves were baseline corrected using capacitive currents.

Electrochemical analysis in bio-electrocatalytical system (BES): The electrodes for BES were prepared in the same way as described above for the electrochemical single cell test. The only difference was that the cathode SGL22B© substrate had dimensions of 4.5 cm×4.5 cm with a circular 5 cm^2 active area coated with Zn/Co–N–C catalyst. The larger dimensions of cathode substrate were

used for a better incorporation into the BES. Also, there was no hot-pressing step carried out and the electrodes were placed on each side of Nafion membrane and assembled in BES.

Microorganism, medium and precultivation: The bacterium *Clostridium ragsdalei* (DSM 15248) was obtained from the German Collection of Microorganisms and Cell Cultures GmbH (DSMZ, Braunschweig, Germany) and stored at −80 °C (10% (v/v) glycerol). The two step precultivation was performed in anaerobic bottles (total volume 500 mL, medium volume 100 mL). Only precultivation medium in anaerobic bottles contained 15 g L^{-1} 2-(N-morpholino)ethanesulfonic acid (MES) as buffer (pH 6). Incubation took place in an incubator (WiseCube WIS-20, Witeg Labortechnik GmbH, Wertheim, Germany) at 37 °C and 100 min^{-1} shaker frequency. 2.5 mL of thawed cell from the glycerol stock were added to the first heterotrophic preculture with 7 g L^{-1} fructose (72 h cultivation time). The second heterotrophic preculture was inoculated by 10 mL from the first preculture. After 24 h it was harvested to serve as the final inoculum. Precultivation and (bio)electrochemical processes were conducted with medium according to Doll et al. (2018).

Liquid product analysis: Bacterial growth was monitored through optical density measurement at a wavelength of λ = 600 nm (OD_{600}) after sampling. OD_{600} was correlated to cell dry weight (CDW) concentrations measured before. Acetic acid concentration was quantified by HPLC (LC-2030 C, Shimadzu, Kyoto, Japan) using a carbohydrate analysis column (Aminex HPX-87H, Bio-Rad, Munich, Germany) and external standards. The system was equipped with a refractive index detector (RID-20 A, Shimadzu, Kyoto, Japan). The analyte eluted isocratically with 5 mM H_2SO_4 and a flow rate of 0.6 mL min^{-1}.

Exhaust gas analysis: Off-gas volume flow was measured by a mass flow meter (F-101D–RAD-33-V, Bronkhorst, Reinach, Switzerland) and a micro gas chromatograph (μ-GC, 490 Micro GC System, Agilent Technologies, Santa Clara, USA) analyzed its composition to determine partial pressures of CO, H_2 and CO_2 (p_{CO}, p_{H2} and p_{CO2}) every 2.5 minutes within the first hour, then every 10 or 30 minutes. CO and H_2 were separated on a molecular sieve column with argon as carrier gas, and 80 °C and 250 kPa. p_{CO2} was measured by a PlotPQ column with helium as carrier gas, 80 °C and 150 kPa. Multiplying the measured partial pressures with the exhaust gas flow rate and integration over time allowed the estimation of total gas production at the cathode.

BES process control: Batch processes were conducted with a working volume of 1 L at 1 bar pressure after autoclaving of the stirred BES at 121 °C. The fermentation medium was anaerobized (2 h, 5 L h^{-1} N_2) before continuous CO_2 purging through a stainless steel frit was started. The gas volume flow was controlled by a gas mixing station (WMR4000, Westphal Mess- und Regeltechnik GmbH, Ottobrunn, Germany) to 1.5 L h^{-1} and the exhaust gas was cooled to 2 °C. Medium temperature (T), pH and stirrer speed (n) were controlled by the bench-top bioreactor station from Infors HT (Infors AG, Bottmingen, Switzerland) to 32 °C, pH 6 and 1200 min^{-1}, and redox potential of the medium was monitored by a probe (ORP Sensor Pt4805-DPAS-SC–K8S/120, Mettler-Toledo GmbH, Gießen, Germany). Potentiostatic chronoamperometry experiments were performend with a potentiostat (Gamry, Reference 3000).

Supporting Information

Supporting info contains the experimental details and additional information on materials characterization and electrochemical testing. The authors have cited additional references within the Supporting Information.[18]

Acknowledgements

Funding by the German Research Foundation (DFG) within the framework of the priority program SPP 2240 (research projects WE 2715/17-1 and FE 1590/1-1) is gratefully acknowledged. The authors thank for the support of Irina Schwarz by the TUM Graduate School. AR thanks Devision 6.1 at BAM for SEM/EDX and XPS measurements. Open Access funding enabled and organized by Projekt DEAL.

Conflict of Interests

The authors declare no conflict of interest.

Keywords: Bioelectrocatalytic CO_2 conversion · CO_2 electrolysis · Autotrophic CO_2 conversion · Atomically dispersed catalysts · PEM electrolysis

[1] S. Hintermayer, S. Yu, J. O. Krömer, D. Weuster-Botz, *Biochem. Eng. J.* **2016**, *115*, 1–13.
[2] S. V. Mohan, J. A. Modestra, K. Amulya, S. K. Butti, G. Velvizhi, *Trends Biotechnol.* **2016**, *34*, 506–519.
[3] N. J. Claassens, C. A. R. Cotton, D. Kopljar, A. Bar-Even, *Nature Catalysis* **2019**, *2*, 437–447.
[4] S. W. Ragsdale, E. Pierce, *Biochim. Biophys. Acta Proteins Proteomics* **2008**, *1784*, 1873–1898.
[5] a) K. Nevin, T. Woodard, A. Franks, Z. Summers, D. Lovley, *mBio* **2010**, *1*; b) K. P. Nevin, S. A. Hensley, A. E. Franks, Z. M. Summers, J. Ou, T. L. Woodard, O. L. Snoeyenbos-West, D. R. Lovley, *Appl. Environ. Microbiol.* **2011**, *77*, 2882–2886; c) T. Zhang, H. Nie, T. S. Bain, H. Lu, M. Cui, O. L. Snoeyenbos-West, A. E. Franks, K. P. Nevin, T. P. Russell, D. R. Lovley, *Energy Environ. Sci.* **2013**, *6*, 217–224; d) H. Nie, T. Zhang, M. Cui, H. Lu, D. R. Lovley, T. P. Russell, *Phys. Chem. Chem. Phys.* **2013**, *15*, 14290–14294; e) N. Faraghiparapari, K. Zengler, *J. Chem. Technol. Biotechnol.* **2017**, *92*, 375–381; f) Z. Zaybak, J. M. Pisciotta, J. C. Tokash, B. E. Logan, *J. Biotechnol.* **2013**, *168*, 478–485.
[6] O. G. Sánchez, Y. Y. Birdja, M. Bulut, J. Vaes, T. Breugelmans, D. Pant, *Curr. Opin. Green Sustain. Chem.* **2019**, *16*, 47–56.
[7] a) J. Wu, T. Sharifi, Y. Gao, T. Zhang, P. M. Ajayan, *Adv. Mater.* **2018**, *31*; b) T. Haas, R. Krause, R. Weber, M. Demler, G. Schmid, *Nature Catalysis* **2018**, *1*, 32–39.
[8] M. Azuma, K. Hashimoto, M. Hiramoto, M. Watanabe, T. Sakata, *J. Electrochem. Soc.* **1990**, *137*, 1772–1778.
[9] a) J. S. Deutzmann, F. Kracke, W. Gu, A. M. Spormann, *Environ. Sci. Technol.* **2022**, *56*, 16073–16081; b) S. T. Boto, B. Bardl, F. Harnisch, M. A. Rosenbaum, *Green Chem.* **2023**, *25*, 4375–4386.
[10] C. G. Giddings, K. P. Nevin, T. Woodward, D. R. Lovley, C. S. Butler, *Front. Microbiol.* **2015**, *6*, 468.
[11] M. Stöckl, T. Lange, P. Izadi, S. Bolat, N. Teetz, F. Harnisch, D. Holtmann, *Biotechnol. Bioeng.* **2023**, *120*, 1465–1477.
[12] a) S. B. Hintermayer, S. Yu, J. O. Krömer, D. Weuster-Botz, *Biochem. Eng. J.* **2016**, *115*, 1–13; b) L. F. M. Rosa, S. Hunger, C. Gimkiewicz, A. Zehnsdorf, F. Harnisch, *Eng. Life Sci.* **2017**, *17*, 77–85; c) T. Krieg, L. M. P. Phan, J. A. Wood, A. Sydow, I. Vassilev, J. O. Krömer, K.-M. Mangold, D. Holtmann, *Biotechnol. Bioeng.* **2018**, *115*, 1705–1716.
[13] a) S. C. Sarma, J. Barrio, A. Bagger, A. Pedersen, M. Gong, H. Luo, M. Wang, S. Favero, C. X. Zhao, Q. Zhang, *Adv. Funct. Mater.* **2023**, *33*, 2302468; b) S. Vijay, W. Ju, S. Brückner, S.-C. Tsang, P. Strasser, K. Chan, *Nature Catalysis* **2021**, *4*, 1024–1031; c) S. D. Rihm, M. K. Kovalev, A. A. Lapkin, J. W. Ager, M. Kraft, *Energy Environ. Sci.* **2023**, *16*, 1697–1710.

[14] D. Menga, F. Ruiz-Zepeda, L. Moriau, M. Šala, F. Wagner, B. Koyutürk, M. Bele, U. Petek, N. Hodnik, M. Gaberšček, T.-P. Fellinger, *Adv. Energy Mater.* **2019**, *9*, 1902412.
[15] A. Mehmood, J. Pampel, G. Ali, H. Y. Ha, F. Ruiz-Zepeda, T.-P. Fellinger, *Adv. Energy Mater.* **2018**, *8*, 1701771.
[16] C. A. Obasanjo, G. Gao, B. N. Khiarak, T. H. Pham, J. Crane, C.-T. Dinh, *Energy Fuels* **2023**, *37*, 13601–13623.
[17] K. Schuchmann, V. Müller, *Nat. Rev. Microbiol.* **2014**, *12*, 809–821.
[18] A. Mehmood, M. Gong, F. Jaouen, A. Roy, A. Zitolo, A. Khan, M.-T. Sougrati, M. Primbs, A. M. Bonastre, D. Fongalland, *Nature Catalysis* **2022**, *5*, 311–323.

Manuscript received: July 18, 2023
Revised manuscript received: November 26, 2023
Version of record online: January 18, 2024